Equilibrium K-, L-, and M-shell ionizations and charge-state distribution of sulfur projectiles passing through solid targets

J. Braziewicz,[1] M. Polasik,[2,*] K. Słabkowska,[2] U. Majewska,[1] D. Banaś,[1] M. Jaskóła,[3] A. Korman,[3] K. Kozioł,[2] W. Kretschmer,[4] and J. Choinski[5]

[1]*Institute of Physics, Jan Kochanowski University, PL-25-406 Kielce, Poland*
[2]*Faculty of Chemistry, Nicholas Copernicus University, PL-87-100 Toruń, Poland*
[3]*The Andrzej Soltan Institute for Nuclear Studies, PL-05-400 Otwock-Świerk, Poland*
[4]*Physikalisches Institut, Universität Erlangen-Nürnberg, D-91058 Erlangen, Germany*
[5]*Heavy Ion Laboratory, Warsaw University, PL-02-097 Warsaw, Poland*

(Received 7 May 2010; published 16 August 2010)

In the present work, an alternative approach for the evaluation of the equilibrium K-, L-, and M-shell ionizations and the mean charge state $\overline{q}$ for projectiles passing through various targets has been proposed. The approach is based on measured K x-ray energy shifts and line intensity ratios and utilizes the theoretical analysis of projectile spectra using multiconfiguration Dirac-Fock calculations. It was applied for the satellite and hypersatellite K lines in the x-ray spectra emitted by sulfur projectiles passing with energies of 9.6–122 MeV through carbon, aluminium, titanium, and iron targets, recorded by a Si(Li) detector. It was found that only in the high projectile energy region there was significant dependence of mean equilibrium K-shell ionization on the target atomic number. The equilibrium L-shell ionization rises with the increase of sulfur energy until 32 MeV, but for higher energies the changes are very weak. The equilibrium M-shell ionization changes very weakly for low projectile energy while for higher energies this ionization is practically constant. For each target, the estimated value of $\overline{q}$ rises with the increase of the sulfur energy value. The dependence of the sulfur charge state on the target atomic number was discussed by taking into account the cross sections for ionization, decay, and electron capture processes. The data were compared with the experimental data measured by other authors and with the predictions of Shima's and Schiwietz and Grande's semiempirical formulas. The presented good agreement points out that this alternative approach delivers quantitative results.

DOI: 10.1103/PhysRevA.82.022709 PACS number(s): 34.50.Fa, 32.30.Rj

I. INTRODUCTION

Knowledge of the charge state of projectiles passing through matter is one of the most relevant questions for studies of ion stopping power and atomic excitation and subsequent material modification during ion-atom interactions. In such processes multiple inner shell vacancies are produced both in the projectile and in the target atoms as the result of collisions. The competition among ionization, excitation, capture, loss of electrons, and decay processes creates an electron-hole equilibrium in the electron shells of the moving projectile which yields the mean equilibrium charge state $\overline{q}$ attained by an ion.

A large number of studies have been performed in this area both experimentally and theoretically. Consequently, there are some well-known reviews concerning projectile charge states such as those by Allison [1] and Betz [2]. Also, extensive tabulations of charge projectile states as well as parameters of the charge distributions are available [1–5]. Theoretically it is known that the ion reaches an equilibrium charge state after penetration of some distance into matter. This charge state $\overline{q}$ is determined by the competition among ionization, excitation, capture, electron loss, and decay processes. Because the mean charge states of the projectile inside matter cannot be determined directly, only the charge states of projectiles emerging from targets have been measured directly using different spectrometers [6–15]. In these papers the relation between ion charge values inside and outside the target is generally open. Simultaneously, two main theoretical models describing the ion charge state in solids have been proposed to answer the question: Is there a significant difference of projectile charge states *inside* and *outside* a solid target? The Bohr and Lindhard (BL) model [16] considers that the fast sequence of collisions experienced by the ion inside a solid produces an enhancement in the ionization and excitation probabilities which increases the equilibrium charge of the ion. Consequently, the projectile charge state inside a solid target increases constantly to the value observed behind the target [16]. According to the Betz and Grodzins (BG) model [17] the effect of sequential ion collisions inside matter produces ions with several excited electrons in outer shells. These electrons are emitted from the projectile immediately after its exit from the target [17,18] when the ion decays to the ground state through Auger processes. The multiple electron emission predicted by this model has been sought for many years [19–22] but the observed number of electrons was much lower. Recently, Lifschitz and Arista [23] have shown, on the basis of adequate nonlinear calculations of the energy loss of heavy ions inside solids using quantum theory to evaluate the transport cross section, that the ion charge inside a solid should be quite close to the charge observed for an ion outside the target.

The problem of the relation between the projectile charge states inside and outside a solid target can be partially explained using x-ray spectra emitted through the projectile being inside and outside of the target. During a collision of an ion with a target atom the strong Coulomb field of one

*mpolasik@uni.torun.pl

 ©2010 The American Physical Society

of the "collision partners" can cause simultaneous ejection of several electrons from the other. This process yields a reduction in the nuclear charge screening and increases the binding energy of the remaining electrons [24]. In a short time the ion reaches an equilibrium inner shell population of electrons which determines the equilibrium charge state of the ion. Finally, as a result of the multiple inner shell ionization, instead of a single-hole x-ray transition called a diagram line, the structure of x-ray satellites appears. Using low-resolution x-ray spectrometers, such as a semiconductor Si(Li) detector, the satellite structure of induced x rays cannot be resolved. Nevertheless, the x-ray spectra are strongly affected by the structure of the inner shell electrons and vacancies. The measured x-ray lines are shifted toward higher energies and broadened with respect to the corresponding x-ray energies of a singly ionized atom [25–27]. Consequently, from these energy shifts and the broadening of K x-ray lines information concerning the probability of multiple ionization can be extracted. The method of analysis of atom multiple ionization applying low-resolution x-ray spectra was used in our previous work to study the ionization probabilities of M, N, and O shells of heavy atoms bombarded by projectiles [28–31] and of K, L, and M shells of sulfur projectiles passing through a carbon target [27,31]. We have used the fact that the x-ray satellite structure can be well approximated by a Gaussian profile whose energy shift and width depend on the K-, L-, and M-shell ionization at the moment of x-ray emission.

Finally, the equilibrium electron configuration of the projectile is achieved as the result of the electron loss and capture processes. The energy of the x rays emitted from such multiply ionized atoms reflects the actual electron population and consequently the total charge state of the projectile during x-ray emission. In our recent work [31,32] it has been shown that the shifts of K x-ray lines with respect to the corresponding x-ray energies of singly ionized atoms are sensitive to the degree of ionization of their L and M shells. On the basis of these experimental x-ray shifts it was possible to estimate the mean equilibrium charge of the projectiles *inside* the solid [33].

The main aim of the present work is the evaluation of the equilibrium K-, L-, and M-shell ionizations, the mean charge state $\overline{q}$, and the charge-state distribution of sulfur projectiles passing (with energies of 9.6–122.0 MeV) through carbon, aluminium, titanium, and iron targets. For this purpose, we have proposed an alternative approach for the evaluation of the equilibrium ionizations of particular shells and the mean charge state for different projectiles passing through various targets. The results were obtained by the analysis of low-resolution sulfur K x-ray spectra using a theoretical model based on multiconfiguration Dirac-Fock (MCDF) calculations. This work is a continuation of our previous study concerning the dynamic formation of K-hole fractions of sulfur projectiles inside a carbon target [27,33,34]. The dependence of sulfur mean charge states $\overline{q}$ on the target atomic number is discussed by taking into account the measured cross sections for ionization, decay, and electron capture processes. Simultaneously, the problem of the ion charge inside and outside of a solid target is discussed. The data for $\overline{q}$ are compared with the semiempirical formulas of Shima *et al.* [35] and Schiwietz and Grande [36]. The universal function allows us to compare $\overline{q}$ results with data measured by the other authors in different ion-target configurations.

II. EXPERIMENTAL DETAILS

The experimental setup was the same as that described earlier [31,34] and therefore only a brief description is presented here. Sulfur ion beams with incident energies of 9.6, 16.0, 22.4, and 32.0 MeV and initial charge states $q = 4^+,6^+$ were obtained from the tandem accelerator at the Institute of Physics of the Erlangen–Nürnberg University and with energies of 65, 79, 99, and 122 MeV and charge states $q = 13^+,14^+$ were extracted from the U-200P cyclotron at the Heavy Ion Laboratory of Warsaw University.

The ion beams passed through two collimators located at 38 and 24 cm in front of the target to define the diameter of the beam spot as 2 mm at the target. The targets (self-supporting foils of different materials) were positioned in a target holder at an angle of 25° to the beam direction. Targets with different effective thicknesses were used: carbon targets of thicknesses in the range of 15–210 μg/cm^2; aluminium foils with thicknesses of 122.4 and 127 μg/cm^2 during the experiment at low sulfur energies (9.6–32.0 MeV) and with thicknesses of 136.8 and 145.6 μg/cm^2 for the high-energy measurements (65–122 MeV); titanium foils with thicknesses 286.4 and 324.5 μg/cm^2 in the low-energy range and 157.8 μg/cm^2 in the high-energy range; and iron foils with thicknesses 180.1, 188.2, 183.2, and 188.7 μg/cm^2, respectively. All the targets were prepared by vacuum evaporation and their absolute thicknesses were determined in separate measurements on the basis of the energy loss of 5.48-MeV α particles emitted by an ^{241}Am source. The necessary values of the stopping power of α particles in the target materials were taken from Biersack and Haggmark [37] and the final target thicknesses were calculated using the computer code TRIM [38]. The target thicknesses were also checked using elastically scattered 2.0-MeV ^{4}He$^+$ ions from the Van de Graaff accelerator of the Institute for Nuclear Studies. The absolute thickness of each target was determined with an accuracy of about ±4%. The targets were considered as "thin" because the ions passing through the foil did not lose an appreciable amount of energy (ΔE was less than $0.15E_0$ for the thickest target at the lowest ion energy and decreased rapidly up to $0.01E_0$ for the highest projectile energy). The estimated self-absorption of the measured x rays in the targets was low and less than 4%. Independent measurements of target thickness enabled absolute normalization of the x-ray intensity on the incident number of projectiles obtained from elastically scattered sulfur ions detected in a silicon surface-barrier detector located inside the chamber at 12.5° to the beam direction.

The K x rays emitted from the moving projectiles were measured by a Si(Li) detector (30 mm^2 active area, crystal thickness of 5 mm, and an energy resolution of FWHM = 150 eV for 6.4 keV) in a reflective geometry at 90° to the beam direction and placed outside the target chamber. The x rays emitted by the projectile passed on their way to the detector through a 10-μm metallized Mylar chamber window, a 25-μm-thick beryllium detector window, and a 5-mm air gap between both windows. Since the registered K x rays were

attenuated due to transmission through the various absorbers the x-ray spectrometer was carefully calibrated to obtain the exact detection efficiency. The calibration was performed according to the recipe of Pajek *et al.* [39] in the x-ray energy range of 1.5–120 keV using standard calibration sources of ^{57}Co, ^{133}Ba, ^{152}Eu, and ^{241}Am and by particle induced x-ray emission (PIXE) measurements of x rays from thin calibration targets ($Z = 13$–42). For the relatively low x-ray energy region (2–5 keV), essential in this work, the detector efficiency was determined to an uncertainty of less than 4%. The energy calibration of the spectrometer (the second sensitive parameter in the present study) was checked several times during the experiment by measuring the x rays emitted from standard radioactive sources (^{57}Co, ^{133}Eu, ^{152}Ba, and ^{241}Am) and was determined with an uncertainty of 2–3 eV depending on the experimental run.

The geometry of the apparatus used in this work means that the detector should register x rays emitted by the projectile inside the target as well as from distances up to 1.2 cm behind the target, so even x rays with different long lifetimes up to 10^{-12} s were registered.

III. METHODOLOGY

A. Spectra analysis procedure

Typical x-ray spectra emitted by sulfur ions passing through the Ti, Al, Fe, and C targets with energies of 9.6, 32.0, 79, and 122 MeV and recorded by the Si(Li) spectrometer are presented in Fig. 1. Depending on the projectile energy, different x-ray lines are resolved in the measured spectra and their origin was described in detail in our previous paper [27]. The $K\alpha^s_{1,2}$, $K\beta^s_{1,3}$ satellite and $K\alpha^h_{1,2}$, $K\beta^h_{1,3}$ hypersatellite peaks are the result of the overlapped contributions corresponding to electron transitions in the sulfur ions of the following types: $1s^{-1} \rightarrow 2p^{-1}$, $1s^{-1} \rightarrow 3p^{-1}$ and $1s^{-2} \rightarrow 1s^{-1}2p^{-1}$, $1s^{-2} \rightarrow 1s^{-1}3p^{-1}$, respectively. For higher incident sulfur energies in a couple of cases the additional hypersatellite peak labeled as Ky^h was detected, which corresponds to the hypersatellite transitions from the $4p$ and $5p$ subshells of excited sulfur (i.e., transitions of the following types: $1s^{-2} \rightarrow 1s^{-1}4p^{-1}$ and $1s^{-2} \rightarrow 1s^{-1}5p^{-1}$). Its presence proves that the Ky^s satellite transitions (i.e., transitions of the following types: $1s^{-1} \rightarrow 4p^{-1}$ and $1s^{-1} \rightarrow 5p^{-1}$) should also take place. The lack of a separate Ky^s satellite peak in the observed spectra indicates [31] that the contribution of this transition type overlaps with another peak and the Ky^s line energy and its intensity were calculated by applying the $K\beta^h_{1,3}$ one according to the procedure described by Majewska *et al.* [31].

The resolved $K\alpha^s_{1,2}$, $K\beta^s_{1,3}$ satellite and $K\alpha^h_{1,2}$, $K\beta^h_{1,3}$, Ky^h hypersatellite peaks in the x-ray spectrum emitted by multiply ionized sulfur projectiles are broadened and shifted toward higher energies (with the width and energy shift being characteristic for individual peaks) in comparison to the $K\alpha_{1,2}$ and $K\beta_{1,3}$ diagram lines of the singly ionized sulfur atom (see Fig. 1). All x-ray peaks recorded by the Si(Li) detector were formed, in fact, by the convolution of the wide (∼150 eV) Gaussian response function of the semiconductor detector with the natural structure of the satellite or hypersatellite lines having typical energy spacing in the range of tens of electron volts. In our previous work (Banaś *et al.* [28]) we showed that assuming a binomial character for the intensity distribution of the x-ray satellites and taking into account their natural widths and their Gaussian energy spread in the semiconductor detector, the measured x-ray peaks appear as a Gaussian profile which is shifted and broadened with respect to the diagram line. Moreover, we have demonstrated [28] that the energy shift and width of each measured x-ray peak can be expressed in terms of the multiple ionization probabilities and the energy shift per electron vacancy. In the present study we adopted this method for the analysis of the measured K x-ray spectra of multiply-ionized sulfur projectiles passing through different foils. The energy and intensity of the resolved x-ray peaks were determined from a least-squares analysis of the spectra using from three to five (see Fig. 1) Gaussian functions (with the characteristic width of the fitting function for each peak) and a polynomial form for the background. The energy shift and width of each x-ray peak reflects the electronic configuration of the highly ionized sulfur projectiles at the time of x-ray emission [27,31].

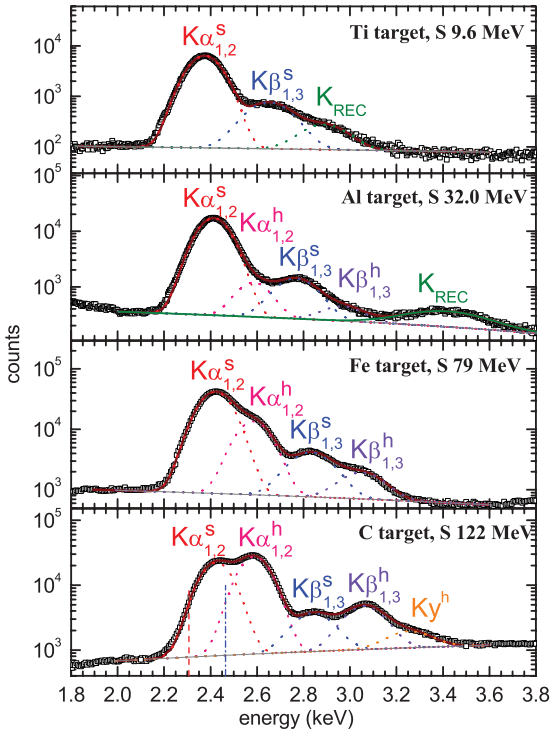

FIG. 1. (Color online) The x-ray spectra emitted by sulfur ions passing through Ti, Al, Fe, and C targets with energies of 9.6, 32.0, 79, and 122 MeV, respectively. Spectra were registered using a Si(Li) detector with FWHM = 150 eV over the energy range 2–4 keV. Dashed and dash-dotted vertical lines show the positions of the sulfur $K\alpha_{1,2}$ and $K\beta_{1,3}$ diagram lines, respectively.

The measured energies of all x rays emitted from the moving ions have been corrected for the Doppler effect, resulting in a transformation of the registered energies into the projectile rest frame. The stopping power of sulfur ions in the target was taken into account by using an effective beam energy. The measured intensities of the x-ray peaks were corrected for the detector efficiency and for self-absorption of x rays in the target [27].

Additionally, x rays emitted as a result of radiative electron capture (REC) from the K, L, and M shells of a target atom to the projectile vacancy form the peak which is marked in Fig. 1 as K_{REC}. Its energy and shape changes drastically with the sulfur projectile energy and also depends on the binding energy of the inner shell electron in the multiply-ionized sulfur [40]. In the sulfur projectile energy range of 9.6–32.0 MeV the energy of the K_{REC} peak is close to the characteristic sulfur K x-ray lines and therefore it was taken into consideration in the peak-fitting procedure. The expected K_{REC} peak form was first simulated to predict its energy and broadening (caused by the distribution of the momenta of the captured electrons according to Biggs *et al.* [41]) for each projectile energy and the data obtained were taken into account as initial parameters in the x-ray peak-fitting procedure. For projectile energies higher than 65 MeV the K_{REC} peak energy in the range 4.6–5.8 keV is far from the analyzed region of the sulfur K x-ray energies and therefore was not taken into account during the fitting procedure.

B. The background of MCDF calculations

In recent years, several theoretical models based on the MCDF method have been developed [42–48] and applied [48–51] to give a reliable description of very complex x-ray spectra accompanying the ionization process. The methodology of the MCDF calculations performed in the present studies is similar to that published earlier (see, e.g., [47]). In this method the Hamiltonian for the N-electron atom is taken to be of the form

$$H = \sum_{i=1}^{N} h_D(i) + \sum_{j>i=1}^{N} C_{ij}, \tag{1}$$

where $h_D(i)$ is the Dirac operator for ith electron and the terms C_{ij} account for electron-electron interactions and come from the one-photon exchange process. The latter are the sum of the Coulomb interaction operator and the transverse Breit operator.

Atomic state functions with total angular momentum J and parity p are represented in the multiconfigurational form

$$\Psi_s(J^p) = \sum_m c_m(s)\Phi(\gamma_m J^p), \tag{2}$$

where $\Phi(\gamma_m J^p)$ are the configuration state functions (CSFs), $c_m(s)$ are the configuration mixing coefficients for state s, and γ_m represent all the information required to uniquely define a certain CSF.

In the present MCDF calculations the energy functional has an identical form to that published in our earlier work [47]. Apart from the transverse (Breit) interaction, two types of quantum electrodynamics (QED) corrections are included, namely the self-energy and vacuum polarization corrections (see McKenzie *et al.* [52]). The formulas for the transition matrix elements and spontaneous emission probabilities can be found in the work of Grant [53]. The calculations were performed for the Coulomb gauge, which yields the dipole velocity expression [53] in the nonrelativistic limit for electric dipole transitions.

It is important to note that the influence of dynamic screening plays some role in the description of ion-solid collisions [54–58]. In such studies the screening length [57] was often used as a simple parameter adequate to qualify the magnitude of the dynamic screening role in such collisions. The preliminary estimations indicate that in our cases the screening lengths have large values (i.e., several times bigger than the impact ion radius), which indicates that not taking the dynamic screening effect into account does not have an important influence on particular subshell ionization values. Therefore, not using this effect in our studies does not cause a visible inaccuracy of the obtained results. Moreover, it seems difficult to apply the concept of dynamic screening for many electron projectiles such as sulfur, because there are no works in the scientific literature which use the dynamic screening for more complicated systems than one electron.

C. Evaluation procedure of the equilibrium K-, L-, and M-shell ionizations and ion charge states

As mentioned, our proposed quantitative approach for the evaluation of the equilibrium K-, L-, and M-shell ionizations and the mean equilibrium charge states $\overline{q}$ of sulfur projectiles is based on the experimental values of various parameters of the K x-ray spectra emitted by the projectiles passing through the target. We have determined the value of the mean charge state $\overline{q}$ according to the following expression:

$$\overline{q} = n_K + n_L + n_M, \tag{3}$$

where n_K is the average number of K-shell vacancies, n_L is the average number of L-shell vacancies, and n_M is the average number of M-shell vacancies.

As seen in Fig. 1, the structure of the measured K x-ray spectra seems very simple, but, in fact, each of the registered K x-ray peaks is composed of many x-ray contributions corresponding to the various types of electronic configurations of sulfur ions. It should be emphasized that, in order to evaluate the equilibrium K-, L-, and M-shell ionizations, and mean charge states $\overline{q}$ of the sulfur projectiles, it was necessary to divide all the measured spectra into two groups dependent on the projectile energy (i.e., 9.6–32.0 and 65–122 MeV) and to apply different approaches for each energy range.

1. Sulfur projectile energies of 9.6–32.0 MeV

For projectiles passing through foils, K-shell ionization is always accompanied by simultaneous multiple ionization of the outer shells. For the low-energy range (9.6, 16.0, 22.4, and 32.0 MeV) we showed in our previous paper [32] that determination of the average number of electron holes in the L and M shells of sulfur projectiles is possible by taking into account the fact that the influence of electron removal from the subshells on the $K\alpha^s_{1,2}$ and $K\beta^s_{1,3}$ transition energies and the $K\beta^s_{1,3} : K\alpha^s_{1,2}$ intensity ratio is nonadditive [32,59]. Specifically, the $K\alpha^s_{1,2}$ and $K\beta^s_{1,3}$ transition energies increase much faster than linearly with the number of holes in a given subshell.

Therefore, to interpret our experimental K x-ray spectra for sulfur, it was necessary [32] to perform theoretical calculations

which take into account simultaneous multiple ionization of the L and M shells. The results of very detailed MCDF calculations for electronic configurations corresponding to various distribution of holes in the $2s$, $2p$, $3s$, and $3p$ subshells of sulfur were presented in our previous paper [32]. From a comparison of these results with all three parameters of the measured sulfur K x-ray spectra (i.e., the $K\alpha^s_{1,2}$ and $K\beta^s_{1,3}$ transition energies and the $K\beta^s_{1,3} : K\alpha^s_{1,2}$ intensity ratio) it was possible to estimate the average number of holes in the M shell (accompanying the L-shell holes). It seems that only those configurations of sulfur in which the average number of M-shell holes is about five can play an important role in the measured K x-ray spectra [27,32]. The average number of M-shell holes slightly increases with the sulfur projectile energy.

a. (L-shell ionization). It is very important to note that the $K\alpha^s_{1,2}$ energy shift strongly depends on the ionization of the $2p$ and $2s$ subshells while the influence of one electron removal from the $3p$ subshell on the $K\alpha^s_{1,2}$ shift is 28 times smaller than from the $2p$ subshell and the influence of one electron removal from the $3s$ subshell is 40 times smaller than from the $2s$ subshell [59]. However, in the case of the $K\beta^s_{1,3}$ energy shift and the $K\beta^s_{1,3} : K\alpha^s_{1,2}$ intensity ratio the difference between the effects of L- and M-shell ionizations is not so large. We have considered here that L-shell ionization means only $2p$ (but not $2s$) subshell ionization because the effect of removing electrons from the $2s$ or $2p$ subshells on the $K\alpha^s_{1,2}$ energy is very similar. Therefore, the difference between the effect of removing electrons from the $2s$ and $2p$ subshells does not provide a significant error. This possible error is practically negligible because the ionization of the $2s$ subshell plays a small role at the time of emission of the K x-ray lines (because the number of electrons in the $2s$ subshell is one-third that in the $2p$ subshell and moreover fast Coster-Kronig transitions cause filling of one hole in the $2s$ shell, creating one hole in the $2p$ shell, simultaneously removing one electron from a higher shell [60]).

In connection with this, we decided to base our determination of the average number of holes in the L shell of the sulfur projectile not on all three parameters of the measured K x-ray sulfur spectra but only on the $K\alpha^s_{1,2}$ energy shift. Therefore, we used the MCDF results for the $K\alpha^s_{1,2}$ energy shift for the initial configurations $1s^{-1}2p^{-3}3s^{-2}3p^{-3}$, $1s^{-1}2p^{-4}3s^{-2}3p^{-3}$, and $1s^{-1}2p^{-5}3s^{-2}3p^{-3}$ of sulfur ions and point out the theoretical dependence of the $K\alpha^s_{1,2}$ energy shift on the number of L-shell vacancies in the presence of five holes in the M shell. This dependence was the basis for the evaluation of the L-shell ionization for different targets and different projectile energies by comparison with the theoretical MCDF and experimental $K\alpha^s_{1,2}$ energy shifts.

b. (M-shell ionization). We have evaluated the average number of M-shell holes by analyzing the dependence of the $K\beta^s_{1,3}$ energy shift values on the number of M-shell holes for a particular L-shell ionization (i.e., for three, four, and five L-shell holes). For three L-shell holes we used the configurations $1s^{-1}2p^{-3}3s^{-1}3p^{-3}$, $1s^{-1}2p^{-3}3s^{-2}3p^{-3}$, and $1s^{-1}2p^{-3}3s^{-2}3p^{-4}4p^1$; for four L-shell holes we used $1s^{-1}2s^{-1}2p^{-3}3s^{-2}3p^{-3}$ and $1s^{-1}2s^{-1}2p^{-3}3s^{-2}3p^{-4}4p^1$; and for five L-shell holes we used $1s^{-1}2p^{-5}3s^{-2}3p^{-3}$ and $1s^{-1}2p^{-5}3s^{-2}3p^{-4}4p^1$. The choice of these configurations corresponds with the conclusion of our previous paper [32] that initial states having a singly occupied $4p$ subshell (instead of a singly occupied $3p$ subshell) can play an important role at the time of emission of the K x-ray spectra from sulfur projectiles passing through solid targets. This is very interesting since the $4p$ subshell is empty in the ground state of the neutral sulfur atom. The average number of holes in the M shell, determined from this procedure, changes from about 5.0 to about 5.4. This confirms that our initial assumption of about five M-shell holes not changing much with the sulfur projectile energy is reasonable and does not introduce any significant errors in the estimation of the average number of L-shell holes.

c. (K-shell ionization). In order to evaluate the K-shell ionization it is necessary to the determine values of particular K-vacancy fractions, which is possible on the basis of the analysis of K-vacancy fraction formation dynamics for sulfur ions passing through various targets [27,34]. In the low-energy region multicollisional effects mainly lead to creation of two fractions of projectiles, that is, a fraction without a K vacancy (F_0) and a fraction with a single K vacancy (F_1). A fraction with a double K vacancy (F_2) only appears at a sulfur energy of 32.0 MeV. In order to evaluate the equilibrium K-shell ionization we have the equation

$$n_K = F_1 + 2F_2. \tag{4}$$

Finally, using Eq. (3), we evaluated the mean charge state $\overline{q}$ for sulfur ions passing with low energies through carbon, aluminium, titanium, and iron targets.

2. Sulfur projectile energies of 65–122 MeV

In the high sulfur projectile energy range (i.e., 65, 79, 99, and 122 MeV) the possible electron configurations are different than in the case of the low-energy range. Each of the K x-ray peaks ($K\alpha^s_{1,2}$, $K\alpha^h_{1,2}$, $K\beta^s_{1,3}$, $K\beta^h_{1,3}$, and Ky^h) is composed of x-ray contributions corresponding to a specific initial configuration of the inner shell electrons [31]. The existence of the $K\alpha^s_{1,2}$ and $K\beta^s_{1,3}$ satellite peaks in the measured x-ray spectra suggests the presence of a fraction of sulfur projectiles with one K-shell hole (F_1) and with an occupied $2p$ or $3p$ subshell, respectively. Similarly, the existence of the $K\alpha^h_{1,2}$ and $K\beta^h_{1,3}$ hypersatellite peaks suggests the presence of a fraction of sulfur projectiles with two K-shell holes (F_2) and with occupied $2p$ and $3p$ subshells, respectively. The last, highest energy peak in the measured spectra labeled as Ky^h (see Fig. 1), which corresponds to the hypersatellite transitions from $4p$ and $5p$ subshells, proves that the corresponding satellite transitions (Ky^s) also take place [34].

Moreover, it was found [31] that five- and more-electron fractions of sulfur ions are negligible in the charge-state distribution for the energies studied and therefore only one-, two-, three-, and four-electron configurations are responsible for the measured x-ray spectra parameters. For possible numbers of electrons we have chosen the configurations which allow the positions of the satellite and hypersatellite peaks to be reproduced and which ensure that these configurations

correspond to the excited states with the lowest energy among all the possible states which can produce the considered peaks [31]. In other words, we assume that the configurations corresponding to the satellite and hypersatellite $K\alpha_{1,2}$, $K\beta_{1,3}$, and Ky peaks have singly occupied $2p$, $3p$, and $4p$ (or $5p$) states, respectively. Consequently, the $K\alpha^s_{1,2}$ and $K\beta^s_{1,3}$ (or $K\alpha^h_{1,2}$ and $K\beta^h_{1,3}$) transitions can be considered independently. The MCDF results show that the possibility of such initial configurations which can de-excitate via $K\alpha^s_{1,2}$ or $K\beta^s_{1,3}$ ($K\alpha^h_{1,2}$ or $K\beta^h_{1,3}$) transitions is negligible.

a. (L- and M-shell ionizations). The number of L- and M-shell holes in the high-energy projectiles can be evaluated on the basis of the x-ray satellite (corresponding to fraction F_1) or hypersatellite (corresponding to fraction F_2) line energy shifts. Consequently, in order to estimate the average L-shell ionization on the basis of the measured satellite $K\alpha^s_{1,2}$ energy shift, we have assumed six M-shell holes (based on the MCDF results) and used the theoretical values for the $K\alpha^s_{1,2}$ shifts corresponding to the following initial configurations of the sulfur ions: $1s^{-1}2s^{-1}2p^{-5}3s^{-2}3p^{-4}$ and $1s^{-1}2s^{-2}2p^{-5}3s^{-2}3p^{-4}$. Finally, we point out the theoretical dependence of the $K\alpha^s_{1,2}$ energy shift on the number of L-shell vacancies. which enables the value of the sulfur L-shell ionization, $n_L^{(K\alpha)}$, inside different targets to be evaluated. In this case the following relation is valid:

$$\overline{q}_{K\alpha} = n_L^{(K\alpha)} + 6 + n_K. \tag{5}$$

Similarly, for the evaluation of the average number of L-shell holes on the basis of the satellite $K\beta^s_{1,3}$ energy shift, $n_L^{(K\beta)}$, we have to assume possible sulfur electronic configurations with five M-shell holes. The MCDF values for the $K\beta^s_{1,3}$ energy shifts corresponding to the configurations $1s^{-1}2s^{-1}2p^{-6}3s^{-2}3p^{-3}$ and $1s^{-1}2s^{-2}2p^{-6}3s^{-2}3p^{-3}$ give the theoretical dependence of the $K\beta^s_{1,3}$ energy shift on the number of L-shell vacancies and allow us to calculate

$$\overline{q}_{K\beta} = n_L^{(K\beta)} + 5 + n_K. \tag{6}$$

Taking into account the $K\beta^s_{1,3} : K\alpha^s_{1,2}$ intensity ratio as

$$x = \frac{I_{K\beta}}{I_{K\alpha}}, \tag{7}$$

where $I_{K\alpha} + I_{K\beta} = 1$, we can evaluate the average number of L- and M-shell holes of the sulfur ions passing with high energies through various targets according to the formulas

$$n_L = \frac{n_L^{(K\alpha)} + x n_L^{(K\beta)}}{1+x}, \tag{8}$$

$$n_M = \frac{6 + x \cdot 5}{1+x}. \tag{9}$$

The L- and M-shell ionizations obtained in the same manner using the hypersatellite $K\alpha^h_{1,2}$ and $K\beta^h_{1,3}$ lines agree with the results obtained on the basis of the satellite lines within an accuracy of 0.3 units of charge.

b. (K-shell ionization). In the high-energy region where the fraction of ions with double K-shell vacancies (F_2) is significant [27,34] the average number of K-shell holes was estimated according to Eq. (4). Finally, we evaluated the mean charge state $\overline{q}$ for sulfur ions passing through targets.

IV. RESULTS AND DISCUSSION

The charge state of the ion changes with the depth of target penetration as a result of electron loss and capture processes. Passing some way into the target, the projectile reaches an equilibrium electron defect configuration in each electron shell, which yields the equilibrium ion charge state. In our previous work [31,32] we have shown that the characteristic parameters of the projectile K x-ray spectra, like x-ray energy and width of different x-ray lines, are sensitive to the degree of inner shell ionization and electron excitation into higher shells. Therefore, the measured x rays inform us about the electronic configuration of the highly ionized projectile at the time of its x-ray emission and enable us to estimate its mean equilibrium charge.

Our previous work [27,31], in which the dependence on carbon target thickness of the experimental energy shifts and the relative intensities of the individual satellite and hypersatellite K x-ray peaks was discussed, sheds light on the problem of electron population equilibration in various shells of sulfur ions. It was shown that the measured shifts of the transition energies for the satellite and hypersatellite $K\alpha^{s,h}_{1,2}$, $K\beta^{s,h}_{1,3}$, and $Ky^{s,h}$ x-ray peaks with respect to the diagram energies for a singly ionized atom [61] are almost (within error bars ~1.5 eV for $K\alpha^{s,h}_{1,2}$, ~3 eV for $K\beta^{s,h}_{1,3}$, and ~4 eV for $Ky^{s,h}$) independent of the target thickness. Generally, this suggests an insignificant role for the nonequilibrium charge fractions of sulfur ions in the L and M shells even in the case of the thinnest carbon foils. The $K\alpha^h_{1,2} : K\alpha^s_{1,2}$ and $K\beta^h_{1,3} : K\beta^s_{1,3}$ intensity ratios allow us to conclude that a rather long path of the projectile inside a carbon target (characteristically increasing with the projectile energy) [27] is required to achieve an equilibrated number of projectile K-shell electrons. We have shown [27] that for the highest sulfur energies equilibration of the electron population in the K shell of the projectile is achieved for the bulk of sulfur ions in a carbon foil with a thickness of not less than 100 μg/cm^2 [27,31].

Moreover, this result is very important as evidence for different charge states of the ion inside (q_{in}) and outside (q_{out}) a solid target. The difference between q_{in} and q_{out} has been widely discussed for years and two main models (BL and BG [16–18]) have been proposed to describe the charge state inside a solid, but neither model is completely suitable. Experimentally, depending on the solid target thickness the fraction of registered x rays originating from the projectile inside and outside the target changes. If a difference of charge states in these two projectile positions existed it would appear in the registered x-ray shifts. No observed dependence of x-ray energy shifts on the target thickness [27,31,33,34] proves the Lifschitz and Arista [23] result, that the ion charge state within a solid should be quite close to the charge observed after the ion exits the target.

The thicknesses of the C, Al, Ti, and Fe targets used during the experiment ($>120\mu$g/cm^2) were chosen to be such that the conditions for equilibration of the electron population in the

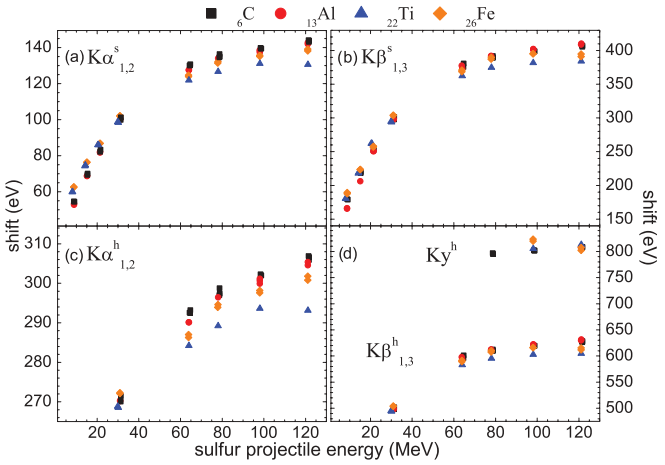

FIG. 2. (Color online) The dependence of the energy shift of the satellite (a) $K\alpha^s_{1,2}$, (b) $K\beta^s_{1,3}$ and hypersatellite (c) $K\alpha^h_{1,2}$, (d) $K\beta^h_{1,3}$, and Ky^h lines of a sulfur projectile on incident energy for various targets.

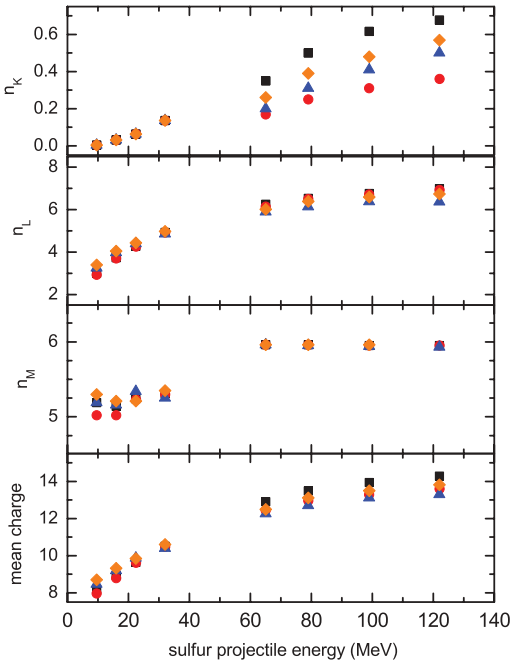

FIG. 3. (Color online) The dependence of evaluated mean equilibrium K-, L-, and M-shell ionization and mean charge of sulfur projectiles on their energy inside solid targets of C (black squares), Al (red circles), Ti (blue triangles), and Fe (orange diamonds).

K, L, and M shell are fulfilled and an equilibrium charge state of the sulfur projectiles will be achieved. In Fig. 2 we present the values of the energy shifts of the $K\alpha^s_{1,2}$, $K\alpha^h_{1,2}$, $K\beta^s_{1,3}$, $K\beta^h_{1,3}$, and Ky^h lines of sulfur ions measured in this work, relative to the diagram energies [61], inside C, Al, Ti, and Fe targets and for all projectile energies. As seen in the figure, the measured energy shifts of all satellite and hypersatellite K x-ray peaks are relatively large and their values increase with increasing sulfur beam energy. Simultaneously, we see that the dependence of the energy shifts on the target atomic number Z_t is relatively weak, but a systematic difference for the various targets is apparent.

A. Equilibrium K-, L-, and M-shell ionization and mean charge $\overline{q}$ of sulfur projectiles

According to the proposed analysis procedure described in Sec. III C the evaluation of the equilibrium K-, L-, and M-shell ionization on the basis of the measured x-ray spectra was possible and the results obtained are presented in Fig. 3 and Table I. In the low projectile energy region we observed no dependence of mean equilibrium K-shell ionization on the target atomic number. In contrast to this, in the higher projectile energy range the dependence on the target atomic number is larger. The equilibrium L-shell ionization rises with increasing incident sulfur energy until 32 MeV. At high projectile energies the L-shell ionization changes very weakly with incident energy. The equilibrium M-shell ionization changes very weakly (from 5.0 to 5.4) in the low projectile energy range while for higher energies this ionization state is practically constant. Finally, the results for the K-, L- and M-shell ionization allowed the mean charge of the projectile passing though the solid target to be evaluated.

The dependence of estimated mean equilibrium charge $\overline{q}$ of sulfur projectiles passing through C, Al, Ti, and Fe targets on the beam energy is graphically presented in Fig. 3. For each target the estimated value of $\overline{q}$ increases with increasing ion energy.

It is worth noticing that the difference between the lowest and the highest value of $\overline{q}$ (for 9.6 and 122 MeV, respectively) for S projectiles passing through C and Al is equal to 6.1 and 5.6 units of charge, respectively. At the same time the estimated mean charge of sulfur traversing Ti and Fe targets is 4.8 and 5.1 units of charge, respectively. The dependence of the $\overline{q}$ value on the target atomic number is generally weak.

Due to be limited experimental data on the charge state of sulfur projectiles moving through different targets we compared the behavior of our results with the charge data for Cl projectiles (a neighboring atom of S) presented by Shima *et al.* [10,12]. Moreover, Shima and co-workers investigated the target atomic number Z_t dependence of charge states of fast Cl ions passing with energies in the range 0.7–3.1 MeV/amu through thin foils of 20 different materials. Their mean charge $\overline{q}$ of Cl ions clearly oscillates as a function of target atomic number Z_t for each projectile energy.

Very good agreement between Shima's results for Cl projectiles and our data for sulfur ions is observed. For the lower energies (0.3–0.7 MeV/amu) the charges $\overline{q}$ of sulfur and chlorine projectiles passing through C and Al targets are lower than the charges of these ions traversing Ti and Fe foils. For 32.0-MeV sulfur and 35.2-MeV chloride projectiles, their charges do not differ much for C, Al, Ti, and Fe foils. In the case of sulfur ions at energies of 65 and 99 MeV and chlorine ions at energies of 68 and 108.5 MeV the $\overline{q}$ values of both projectiles is higher when these projectiles pass through

TABLE I. The dependence of evaluated mean equilibrium K-, L-, and M-shell ionization and mean charge of sulfur projectiles (passing through solid targets of C, Al, Ti, and Fe) on their energy.

		Projectile energy (MeV)							
	Target	9.6	16.0	22.4	32.0	65	79	99	122
n_K	C	0.004 ± 0.0004	0.03 ± 0.003	0.06 ± 0.006	0.14 ± 0.01	0.35 ± 0.04	0.50 ± 0.05	0.62 ± 0.06	0.68 ± 0.07
	Al	0.004 ± 0.0004	0.03 ± 0.003	0.06 ± 0.006	0.14 ± 0.01	0.17 ± 0.02	0.25 ± 0.03	0.31 ± 0.03	0.36 ± 0.04
	Ti	0.004 ± 0.0004	0.03 ± 0.003	0.06 ± 0.006	0.14 ± 0.01	0.20 ± 0.02	0.31 ± 0.04	0.41 ± 0.04	0.50 ± 0.05
	Fe	0.004 ± 0.0004	0.03 ± 0.003	0.06 ± 0.006	0.14 ± 0.01	0.26 ± 0.03	0.38 ± 0.04	0.48 ± 0.04	0.57 ± 0.06
n_L	C	3.0 ± 0.1	3.7 ± 0.1	4.3 ± 0.1	4.9 ± 0.1	6.3 ± 0.3	6.5 ± 0.2	6.8 ± 0.2	7.0 ± 0.3
	Al	2.9 ± 0.1	3.7 ± 0.1	4.3 ± 0.1	4.9 ± 0.1	6.2 ± 0.4	6.5 ± 0.4	6.7 ± 0.4	6.9 ± 0.4
	Ti	3.3 ± 0.1	4.0 ± 0.1	4.4 ± 0.1	4.9 ± 0.1	5.0 ± 0.4	6.2 ± 0.4	6.4 ± 0.4	6.4 ± 0.4
	Fe	3.4 ± 0.1	4.0 ± 0.1	4.4 ± 0.1	5.0 ± 0.1	6.0 ± 0.4	6.4 ± 0.4	6.6 ± 0.4	6.7 ± 0.4
n_M	C	5.2 ± 0.1	5.1 ± 0.1	5.2 ± 0.1	5.3 ± 0.1	6.0 ± 0.1	6.0 ± 0.1	6.0 ± 0.1	6.0 ± 0.1
	Al	5.0 ± 0.1	5.0 ± 0.1	5.2 ± 0.1	5.3 ± 0.1	6.0 ± 0.1	6.0 ± 0.1	6.0 ± 0.1	6.0 ± 0.1
	Ti	5.2 ± 0.1	5.2 ± 0.1	5.3 ± 0.1	5.3 ± 0.1	6.0 ± 0.1	6.0 ± 0.1	5.9 ± 0.1	5.9 ± 0.1
	Fe	5.3 ± 0.1	5.2 ± 0.1	5.3 ± 0.1	5.4 ± 0.1	6.0 ± 0.1	6.0 ± 0.1	6.0 ± 0.1	6.0 ± 0.1
$\overline{q}$	C	8.2 ± 0.1	8.9 ± 0.2	9.6 ± 0.1	10.5 ± 0.2	12.9 ± 0.3	13.5 ± 0.2	14.0 ± 0.2	14.3 ± 0.3
	Al	8.0 ± 0.1	8.8 ± 0.1	9.6 ± 0.1	10.5 ± 0.1	12.5 ± 0.4	13.0 ± 0.4	13.3 ± 0.4	13.6 ± 0.4
	Ti	8.5 ± 0.1	9.2 ± 0.1	9.9 ± 0.1	10.4 ± 0.1	12.3 ± 0.4	12.7 ± 0.4	13.1 ± 0.4	13.3 ± 0.4
	Fe	8.7 ± 0.1	9.3 ± 0.1	9.9 ± 0.1	10.6 ± 0.1	12.5 ± 0.4	13.1 ± 0.4	13.5 ± 0.4	13.8 ± 0.4

carbon and aluminium targets than for titanium and iron. For both kinds of ions $\overline{q}$ reaches a minimum value for Ti foils. The dependence of $\overline{q}$ on Z_t and projectile energy will be discussed in the following in the light of projectile excitation, ionization, decay, and electron capture processes.

In recent years semiempirical formulas for projectile charge $\overline{q}$ traversing matter have been obtained by several authors [19,62–68]. These formulas include the target atomic number dependence and cover a broad ion energy region. A widely used universal formula proposed by Shima *et al.* [35] is as follows:

$$\begin{aligned}\overline{q}/Z_p &= [1 - \exp(-1.25X + 0.32X^2 - 0.11X^3)] \\ &\quad \times [1 - 0.0019(Z_t - 6)\sqrt{X} + 0.00001(Z_t - 6)^2 X] \\ &= [\overline{q}/Z_p(Z_t = 6)][1 + g(Z_t)], \end{aligned} \tag{10}$$

where Z_p and Z_t denote the ion and target atomic numbers, respectively, and X is the reduced ion velocity defined by Nikolaev and Dmitriev [62] as $X = v_p/[3.6 \times 10^8\ (\mathrm{cm/s}) Z_p^{0.45}]$, where v_p is the projectile velocity. The factor $1 - \exp(-1.25X + 0.32X^2 - 0.11X^3)$ was obtained on the basis of the most abundant charge-state distribution of ions traversing carbon foils.

A multiparameter least-squares fit formula for mean equilibrium charge states of projectiles ranging from protons to uranium has been also presented by Schiwietz and Grande [36] on the basis of about 850 experimental points as

$$\overline{q} = Z_p[(12x + x^4)/(0.07/x + 6 + 0.3x^{0.5} + 10.37x + x^4)], \tag{11}$$

with $x = (v_p/v_0 Z_p^{-0.52} Z_t^{-0.019 Z_p^{-0.52} v_p/v_0}/1.68)^{1+1.8/Z_p}$, where v_0 is the Bohr velocity.

A comparison between the $\overline{q}$ values measured in this work with the data predicted by the Shima and Schiwietz-Grande formulas is presented in Fig. 4. Our experimental data are best described over the full energy range by Schima's formula in the case of C targets and by Schiwietz-Grande's formula in the case of Al targets. The largest disagreement between experimental data and Shima's and Schiwietz-Grande's formulas is observed for the Ti targets at the lowest and largest values of ion energies and is as large as ~13%. The same disagreement is observed in the case of Fe targets at the lowest sulfur ion energy.

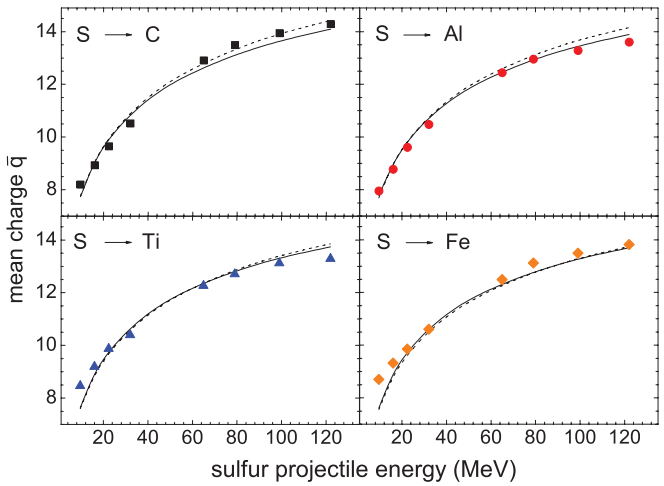

FIG. 4. (Color online) Evaluated "experimental" mean charge $\overline{q}$ values (square, circle, triangle, and diamond symbols) and data estimated on the basis of Shima's [dashed line, Eq. (10)] and Schiwietz's [solid line, Eq. (11)] formulas for C, Al, Ti, and Fe targets as a function of sulfur projectile energy.

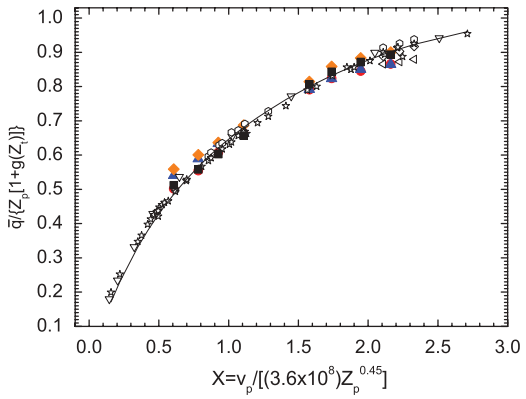

FIG. 5. (Color online) Evaluated "experimental" mean equilibrium charge state $\overline{q}$ of sulfur projectiles passing through C (black squares), Al (red circles), Ti (blue triangles), and Fe (orange diamonds) targets plotted on the universal curve $\overline{q}/\{Z_p[1+g(Z_t)]\}$ vs reduced velocity of ions. The curve denotes the empirical formula of Shima [35]. The data from Refs. [3–5] for S and Cl projectiles passing through Be, C, Al, Ni, and C targets are denoted by the open black symbols.

In Fig. 5 the experimental data are presented in coordinates $\overline{q}/\{Z_p[1+g(Z_t)]\}$ versus reduced ion velocity X, which, according to the fitting procedure of Schima, is a universal behavior of mean equilibrium ion charge state passing through Z_t foils. In this figure the other experimental data for sulfur ions passing through Be, C, Al, and Ni targets [35] and data for chlorine projectiles passing through C foils [3–5] are compared with our data and the universal function of Schima. The best agreement between our experimental values of $\overline{q}$ and Schima's universal estimation is observed for C targets. These data reflect the universal curve with an accuracy of about $\sim$1% and in this case the dispersion of the data is about 0.2 units of charge. The greatest disagreement is observed for the lowest sulfur energy in Ti and Fe targets and is not higher than 0.7 units of charge and for the highest ion energy in Al and Ti targets on the level of 0.4 units of charge.

The results obtained are in good agreement with the conclusion of Schiwietz and Grande [36]. It is emphasized that they found no remaining systematic single-parameter dependence between the experimental values of ion charge state and ion velocity or the nuclear charges of the ion and target. In fact, the observed small disagreement of the present data with the fitted values appears to be consistent with the deviation of experimental data taken from different laboratories. According to Schiwietz and Grande, a comparison between the predictions of Eq. (11) and experimental data indicates that "other hidden" parameters influence the value of $\overline{q}$. There exists some remaining systematic single parameter dependence of $\overline{q}_{\rm expt} - \overline{q}_{\rm fit}$ on the mean number of bound projectile electrons ($N_b = Z_p - \overline{q}$) [36]. In relation to this conclusion, for the low-energy region, when the mean number of bound sulfur electrons is as large as eight our experimental values of $\overline{q}$ are statistically greater than the fitted data by as much as about 0.5 units of charge. At higher projectile energies, when the mean number of bound electrons is much lower than six the experiment-to-fit agreement is satisfactory, although the dispersion of the experimental data is about 0.5 units of charge and the observed disagreements at the highest sulfur energies are inside this "experimental dispersion."

The good agreement of our data with the other data presented in Figs. 4 and 5 and the semiempirical estimations points out that the method used in the present work delivers qualitative results concerning the charge states of ions traversing solid targets. Additionally, the great merit of this method is the possibility of estimating the inner shell equilibrium ionization of an ion inside a solid target using a low-resolution x-ray semiconductor detector.

These results prove the opinion that other hidden parameters may influence the value of the projectile charge $\overline{q}_{\rm expt}$. As mentioned before, the average charge of the projectile is a result of electron loss and capture processes which the projectile has undergone passing through matter. Therefore, in the present paper we tried to look for the influence of ionization and electron capture processes on the charge state of the ion. In order to explain the origin of the projectile charge dependence on the target atomic number and ion energy, the ionization and electron capture cross sections have been estimated. Cross sections for direct K- and L-shell ionization of sulfur ions by target atoms of carbon, aluminium, titanium, and iron were calculated using the plane-wave Born approximation (PWBA) model [69] and the total ionization cross section was obtained. The electron capture processes were described using the Oppenheimer-Brinkmann-Kramers (OBK) formulation described by Nikolaev [70] and by Lapicki and McDaniel [71]. These calculations enabled the total electron capture cross section from K, L, M, and N shells of the target atoms to the inner shells of the sulfur projectile with an appropriate number of vacancies [27,31] obtained on the basis of multiconfiguration Dirack-Fock calculations to be estimated [47]. In contrast to the work of Gardner *et al.* [72] or Cocke *et al.* [73] no scaling factor was introduced to the calculated cross section values. The theoretical estimations for ionization and electron capture were performed for "realistic" K-, L-, and M-shell binding energies, expected for the most probable configurations of multiply ionized sulfur projectiles [31,32], calculated using the multiconfiguration Dirack-Fock method [47].

Over the energy range of sulfur projectiles used here the K- and L-shell vacancy production processes are dominated by Coulomb ionization and the value of these cross sections (and the total ionization cross section) increases homogeneously with increasing target atomic number. Consequently, the observed dependence of the mean projectile charge on target atomic number [10,12] should be dominated by the electron capture process. In the present paper we tried to consider the influence of electron loss from K and L projectile shells and capture of K-, L-, M-, and N-shell target atom electrons into the K, L, and M shells of the sulfur projectile on the projectile mean charge state. Shima and co-workers [10,12] suggested that one of the origins of the projectile charge dependence on the target atomic number Z_t is the dependence of the electron capture cross section on the projectile inner shell vacancies. In Fig. 6 the mean charges $\overline{q}$ of sulfur projectiles measured in this work are plotted as a function of target atomic number Z_t together with the total electron capture cross section to the sulfur inner vacancies ($\sigma_{\rm EC}^{\rm tot}$). Also presented are values of the

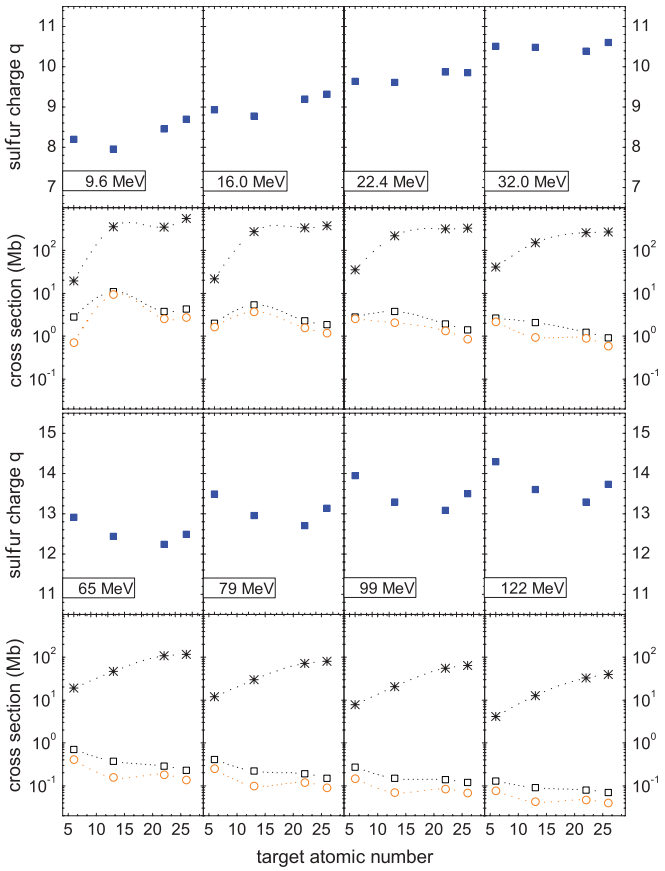

FIG. 6. (Color online) The dependence of the sulfur mean equilibrium charge state (blue squares), total electron capture cross section (black asterisks), the ratio of the total electron capture to the total ionization cross section (black open squares), and the ratio of the L-shell electron capture to the L-shell ionization (orange open circles) cross section on the target atomic number.

ratio of total electron capture cross section to total ionization cross section, $\sigma_{\rm ion}^{\rm tot}$, and the ratio of the cross section for electron capture to the L-shell to L-shell ionization, $\sigma_{\rm EC}^{L}/\sigma_{\rm ion}^{L}$, for the studied sulfur energies.

In the lowest projectile energy region, the contribution of $\sigma_{\rm EC}^{K}$ (i.e., electron capture into the sulfur K shell from the K, L, M, and N shells of the atom target) to the total electron capture cross section $\sigma_{\rm EC}^{\rm tot}$ is significantly lower than that into L- and M-shell vacancies and these data determine the $\sigma_{\rm EC}^{\rm tot}$ value. In this low sulfur projectile energy region the value of $\sigma_{\rm EC}^{\rm tot}$ shows the largest dependence on the target atomic number. Additionally, $\sigma_{\rm EC}^{\rm tot}$ dominates over the value of the ionization cross section and consequently its dependence on target atomic number Z_t is the main influence on the value of the ion charge state. Its maximum value observed for Al targets correlates with the minimum value of sulfur charge traversing this target. Concluding, we observed a good correlation between the dependence of the sulfur charge and the ratio of the total electron capture to the total sulfur ionization cross sections on the target atomic number (see the upper rows of Fig. 6). In the mid-energy range (i.e., 22.4–32.0 MeV) the values of the ionization and electron capture cross sections are equivalent and the behavior of these data is very weakly dependent on the target atomic number as well as the equilibrium sulfur charge. The dependence of $\overline{q}$ on Z_t and $\sigma_{\rm EC}^{\rm tot}/\sigma_{\rm ion}^{\rm tot}$ on Z_t disappears with increasing ion energy.

The L-shell ionization process dominates over the total electron capture process in the highest incident ion energy region (i.e., over 60 MeV). In this case we observe that $\sigma_{\rm EC}^{\rm tot}/\sigma_{\rm ion}^{\rm tot} < 1$, which means the domination of loss processes over the electron capture process in sulfur projectiles. Consequently, in this energy regime the mean sulfur charge is dependent on the target atomic number in the same manner as the value of the ratio $\sigma_{\rm EC}^{L} : \sigma_{\rm ion}^{L}$.

B. Charge-state distribution of sulfur projectiles

The equilibrium charge-state distributions for sulfur projectiles inside solid targets may be estimated on the basis of data for sulfur charges. According to Schima *et al.* [4] the equilibrium charge fractions $F(q)$ have been deduced using the measured projectile charges $\overline{q}$ and their charge distribution widths w according the Gaussian distribution

$$F(q) = (1/\sqrt{2\pi}\,w)\exp[-(q-\overline{q})^2/2w^2]. \qquad (12)$$

The width distribution w was obtained from the experimental data collected by Shima *et al.* [5]. Limited data for the charge distribution width w for sulfur projectiles with energies of 116, 129.4, and 141.8 MeV in Be, C, Al, and Ni targets showed that the value of the width w does not depend strongly (~10%) on the target atomic number Z_t. Moreover, for chlorine projectile energies ~20–120 MeV, the value of the charge distribution width w does not change as a function of target atomic number 4–28 (Be, C, Mg, Al, Ti, Cr, Fe, Ni, and Ge) to within an uncertainty of 2% to 12%, respectively [5]. Since the mean charges of sulfur and chlorine ions emerging from C (see [4,5]) and Al, Ti, and Fe targets are very similar it is reasonable to assume that the width of the charge distribution, w, of sulfur projectiles traversing solid material depends very weakly on the target atomic number Z_t. According to the approach by Shima *et al.* [4] we have assumed the charge distribution width w for sulfur ions inside all the targets studied here (Al, Ti, Fe) to be equal to that for a carbon target.

The second approach used in our work is that of Schiwietz and Grande [36]. They defined a reduced width of the charge-state distribution as

$$w = dZ_p^{-0.27}Z_t^{0.035-0.0009Z_p}f(\overline{q})f(Z_p-\overline{q}), \qquad (13)$$

with $f(x) = \sqrt{(x+0.37Z_p^{0.6})/x}$ and $d = [\Sigma(q-\overline{q})^2F(q)]^{1/2}$. The $Z_p^{-0.27}$ dependence dominates the general trend of the data and the function f serves as a correction for the statistical reduction of the width at either very low or very high mean charge states [36]. The values of w obtained on the basis of Shima's data are higher from ~40% for the highest projectile energies to ~24% for the lowest ion energies in comparison to the values calculated by means of Schiwietz-Grande's recipe. The width w of the charge distribution adopted from Shima's data for carbon targets

decreases smoothly with increasing projectile energy [with the difference being equal to ∼21% for the lowest (9.6 MeV) and the highest (122 MeV) energies]. The reduced width w obtained on the basis of Schiwietz and Grande's formula depends on Z_t and the dependence on ion energy is different for different targets: It is strongest for Ti targets and weakest for Al foils (with 14% and 4% difference in value for energies of 9.6 and 122 MeV).

TABLE II. The evaluated "experimental" equilibrium charge-state distribution according to Shima *et al.* [4] and according to Schiwietz and Grande [36] of sulfur ions passing through (a) carbon, (b) aluminium, (c) titanium, and (d) iron foils. ($\overline{q}$ is the mean equilibrium charge of the ions.)

(a) C target: Charge state fraction of S ions at various energies (MeV)

	According to Shima *et al.* [4]								According to Schiwietz and Grande [36]							
	9.6	16.0	22.4	32.0	65	79	99	122	9.6	16.0	22.4	32.0	65	79	99	122
$\overline{q}$	8.2	8.9	9.6	10.5	12.9	13.5	13.9	14.3	8.2	8.9	9.6	10.5	12.9	13.5	13.9	14.3
6+	0.057	0.014	0.002						0.005							
7+	0.201	0.085	0.024	0.003					0.134	0.013						
8+	0.339	0.250	0.124	0.029					0.541	0.237	0.037	0.001				
9+	0.271	0.346	0.299	0.144					0.298	0.563	0.375	0.056				
10+	0.103	0.225	0.333	0.321	0.008				0.022	0.179	0.498	0.437				
11+	0.019	0.069	0.172	0.324	0.071	0.019	0.004			0.008	0.087	0.446	0.013	0.001		
12+	0.002	0.010	0.041	0.147	0.261	0.133	0.053	0.018			0.002	0.059	0.242	0.056	0.010	0.002
13+			0.005	0.030	0.382	0.352	0.255	0,160				0.001	0.573	0.450	0.223	0.101
14+				0.003	0.222	0.348	0.415	0.418					0.166	0.441	0.580	0.528
15+					0.051	0.129	0.228	0.324					0.006	0.052	0.180	0.340
16+					0.005	0.018	0.042	0.074						0.001	0.007	0.027

(b) Al target: Charge state fraction of S ions at various energies (MeV)

	According to Shima *et al.* [4]								According to Schiwietz and Grande [36]							
	9.6	16.0	22.4	32.0	65	79	99	122	9.6	16.0	22.4	32.0	65	79	99	122
$\overline{q}$	8.0	8.8	9.6	10.5	12.4	13.0	13.3	13.6	8.0	8.8	9.6	10.5	12.4	13.0	13.3	13.6
6+	0.082	0.019	0.002						0.014							
7+	0.244	0.105	0.025	0.003					0.228	0.025	0.001					
8+	0.344	0.276	0.129	0.031					0.554	0.308	0.044	0.001				
9+	0.230	0.341	0.303	0.149	0.002				0.195	0.531	0.388	0.064				
10+	0.073	0.198	0.330	0.325	0.025	0.005	0.001		0.010	0.130	0.481	0.447	0.001			
11+	0.011	0.054	0.166	0.320	0.147	0.060	0.024	0.007		0.005	0.084	0.429	0.067	0.011	0.002	
12+	0.001	0.007	0.039	0.142	0.350	0.251	0.168	0.094			0.002	0.057	0.469	0.222	0.101	0.040
13+			0.004	0.028	0.331	0.396	0.397	0,356				0.001	0.415	0.571	0.529	0.402
14+				0.003	0.125	0.232	0.316	0.397					0.046	0.188	0.341	0.486
15+					0.019	0.051	0.085	0.131					0.001	0.008	0.027	0.071
16+					0.001	0.004	0.008	0.013								0.001

(c) Ti target: Charge state fraction of S ions at various energies (MeV)

	According to Shima *et al.* [4]								According to Schiwietz and Grande [36]							
	9.6	16.0	22.4	32.0	65	79	99	122	9.6	16.0	22.4	32.0	65	79	99	122
$\overline{q}$	8.4	9.2	9.9	10.4	12.2	12.7	13.1	13.3	8.4	9.2	9.9	10.4	12.2	12.7	13.1	13.3
6+	0.036	0.007	0.001						0.002							
7+	0.156	0.057	0.015	0.004					0.073	0.006						
8+	0.318	0.203	0.091	0.037					0.449	0.143	0.020	0.002				
9+	0.309	0.342	0.262	0.167	0.003				0.416	0.531	0.267	0.088				
10+	0.142	0.271	0.348	0.336	0.038	0.011	0.002		0.058	0.295	0.542	0.483	0.003			
11+	0.031	0.101	0.214	0.306	0.189	0.095	0.036	0.018	0.001	0.024	0.163	0.382	0.116	0.026	0.003	
12+	0.003	0.018	0.061	0.125	0.373	0.311	0.210	0.160			0.007	0.043	0.543	0.345	0.143	0.074
13+		0.001	0.008	0.023	0.293	0.379	0.413	0.418				0.001	0.315	0.533	0.595	0.576
14+				0.002	0.092	0.172	0.273	0.324					0.023	0.094	0.248	0.334
15+					0.011	0.029	0.061	0.074						0.002	0.010	0.015
16+					0.001	0.002	0.005	0.005								

TABLE II. (*Continued*.)

(d) Fe target: Charge state fraction of S ions at various energies (MeV)

	According to Shima *et al.* [4]								According to Schiwietz and Grande [36]							
	9.6	16.0	22.4	32.0	65	79	99	122	9.6	16.0	22.4	32.0	65	79	99	122
$\overline{q}$	8.7	9.3	9.9	10.6	12.5	13.1	13.5	13.8	8.7	9.3	9.9	10.6	12.5	13.1	13.5	13.8
6+	0.022	0.005	0.001						0.001							
7+	0.117	0.045	0.015	0.002					0.036	0.003						
8+	0.287	0.179	0.094	0.024					0.345	0.106	0.021	0.001				
9+	0.333	0.334	0.265	0.128	0.001				0.502	0.497	0.277	0.048				
10+	0.183	0.291	0.347	0.309	0.022	0.003	0.001		0.112	0.354	0.537	0.391	0.001			
11+	0.048	0.119	0.210	0.334	0.138	0.043	0.014	0.003	0.004	0.038	0.157	0.474	0.059	0.006	0.001	
12+	0.006	0.023	0.059	0.163	0.343	0.213	0.124	0.059		0.001	0.007	0.084	0.446	0.158	0.053	0.014
13+		0.002	0.008	0.036	0.340	0.393	0.365	0.292				0.002	0.437	0.563	0.452	0.280
14+				0.004	0.134	0.270	0.361	0.432					0.055	0.258	0.443	0.580
15+					0.021	0.069	0.121	0.189					0.001	0.015	0.050	0.123
16+					0.001	0.007	0.014	0.024						0.001		0.003

The values of the mean charge $\overline{q}$ and the equilibrium charge-state distributions of sulfur ions passing through C, Al, Ti, and Fe targets obtained according to both approaches (by Shima *et al.* [4] and by Schiwietz and Grande [36]) are presented in Table II. Moreover, Fig. 7 shows the equilibrium charge-state distributions for selected sulfur energies. It is known that the charge equilibrium for the projectile in the target is the result of a few competitive processes. The obtained charge-state distribution shows the smaller absolute target dependence at 9.6 MeV projectile energy than at 122 MeV (see Fig. 7), while the relative dependence of the mean charge $\overline{q}$ on the kind of target is different (achieving 9% at 9.6 MeV and decreasing to 7% at 122 MeV; see the numerical values in Table I). It seems that the target electronic structure is less important in determining the projectile charge states at higher energies.

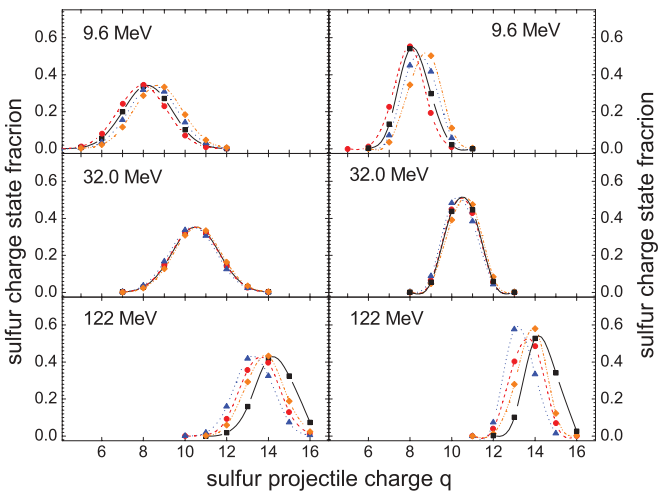

FIG. 7. (Color online) The dependence of the evaluated "experimental" charge state fractions on target atomic number for sulfur projectiles at 9.6, 32.0, and 122 MeV energies passing through C (black squares), Al (red circles), Ti (blue triangles), and Fe (orange diamonds), estimated on the basis of Shima's [4] (left side) and Schiwietz and Grande's [36] (right side) approximations.

V. SUMMARY AND CONCLUSIONS

In the present work, an alternative approach for the evaluation of the equilibrium K-, L-, and M-shell ionizations, mean charge state $\overline{q}$, and charge-state distribution for projectiles passing through various targets has been proposed. The approach is based on the measured K x-ray energy shifts and x-ray line intensity ratios, and it utilizes a theoretical analysis of projectile K x-ray spectra using multiconfiguration Dirac-Fock calculations.

This method has been applied to the satellite and hypersatellite K x-ray lines emitted by sulfur projectiles passing with energies of 9.6–122 MeV through carbon, aluminium, titanium, and iron targets recorded by a Si(Li) detector. The measured energy shifts of all satellite and hypersatellite K x-ray peaks (with respect to the corresponding diagram lines) are relatively large and their values grow with increasing sulfur projectile energy. Simultaneously, it was pointed out that the dependence of the energy shifts on the target atomic number Z_t is relatively weak, but a systematic difference has been observed.

According to the proposed procedure, the equilibrium K-, L-, and M-shell ionizations were obtained and were the basis for an evaluation of the mean charge state $\overline{q}$. The data were compared with the experimental data measured by other authors and with the predictions of Shima's and Schiwietz and Grande's semiempirical formulas. The good agreement obtained suggests that this method delivers quantitative results. Additionally, the great merit of the method is that it answers the very important aspect of the difference between ion charge states inside and outside a solid target. The results of this work settled this question, showing that the ion charge within a solid should be quite close to the ion charge just after its exit.

Some general conclusions can be drawn on the basis of our study. In the case of a small energy range of the projectile (i.e., 9.6–32.0 MeV), we found that (i) the average number of holes in the L shell of the sulfur projectile strongly rises with increasing energy; (ii) in contrast, the average number of holes in the M shell slightly increases, from about 5.0 to about 5.4, with rising projectile energy; (iii) initial states

having one electron in the $4p$ subshell can appear; and (iv) generally, the average number of holes in the L and M shells weakly depends on the target atomic number Z_t. In the case of the higher ion energy range of 65–122 MeV, the general conclusions are (i) the average number of holes in the L and M shells is practically independent of the ion energy and (ii) the ion charge state is determined by the statistical distribution of only a few electrons.

The dependence of the sulfur projectiles' mean charge state $\overline{q}$ on the target atomic number was discussed by taking into account the data of the cross sections for ionization, decay, and electron capture processes. In the low sulfur projectiles energy region, the dependence of the ion mean charge on the atomic number of the solid target is dominated by the ratio of the total electron capture to the total ionization cross section. In the large projectile energy region, the mean sulfur charge is dependent on the target atomic number in the same manner as the value of the L-shell electron capture to the ionization cross section ratio $\sigma_{\mathrm{EC}}^{L} : \sigma_{\mathrm{ion}}^{L}$.

Concluding, in the present paper we proposed a quantitative approach enabling a reasonable estimation of the equilibrium K-, L-, and M-shell ionizations and the mean charge state $\overline{q}$ for ions passing through solid targets.

ACKNOWLEDGMENTS

This work was supported by the Polish Ministry of Science and Higher Education under Grant No. N N202 1465 33. We wish to express our appreciation to the staff of the U-200P cyclotron at the Heavy Ion Laboratory of Warsaw University and the staff of the tandem accelerator of Erlangen–Nürnberg University for their kind collaboration during the measurements. We thank Dr. N. Keeley for a critical reading of the manuscript and for constructive suggestions.

[1] S. K. Allison, Rev. Mod. Phys. B **30**, 1137 (1958).
[2] H. D. Betz, Rev. Mod. Phys. B **44**, 465 (1972).
[3] A. B. Wittkower and H. D. Betz, At. Data **5**, 113 (1973).
[4] K. Shima, N. Kuno, M. Yamanouchi, and H. Tawara, At. Data Nucl. Data Tables **51**, 173 (1992).
[5] K. Shima, T. Mikumo, and H. Tawara, At. Data Nucl. Data Tables **34**, 357 (1986).
[6] C. D. Moak, H. O. Lutz, L. B. Bridwell, L. C. Northliffe, and S. Datz, Phys. Rev. **176**, 427 (1968).
[7] F. Bell, H. D. Betz, H. Panke, W. Stehling, and E. Spindler, J. Phys. B **9**, 3017 (1976).
[8] W. N. Lennard and D. Phillips, Phys. Rev. Lett. **45**, 176 (1980).
[9] T. Ishihara, K. Shima, T. Kimura, S. Ishii, T. Momoi, H. Yamaguchi, K. Umetani, M. Moriyama, M. Yamanouchi, and T. Mikumo, Nucl. Instrum. Methods **204**, 235 (1982).
[10] K. Shima, T. Ishihara, T. Momoi, T. Miyoshi, K. Numata, and T. Mikumo, Phys. Lett. A **98**, 106 (1983).
[11] K. Shima, T. Ishihara, T. Miyoshi, T. Momoi, and T. Mikumo, Phys. Rev. A **29**, 1763 (1984).
[12] K. Shima, Nucl. Instrum. Methods Phys. Res. B **10-11**, 45 (1985).
[13] K. Shima, E. Nakagawa, T. Kakita, M. Yamanouchi, Y. Awaya, T. Kambara, T. Mizogawa, and Y. Kanai, Nucl. Instrum. Methods Phys. Res. B **33**, 212 (1988).
[14] K. Shima, N. Kuno, T. Kakita, and M. Yamanouchi, Phys. Rev. A **39**, 4316 (1989).
[15] K. Shima, N. Kuno, and M. Yamanouchi, Phys. Rev. A **40**, 3557 (1989).
[16] N. Bohr and J. Lindhard, K. Dan. Vidensk. Selsk. Mat. Fys. Medd. **28**, 1 (1954).
[17] H. D. Betz and L. Grodzins, Phys. Rev. Lett. **25**, 211 (1970).
[18] H. D. Betz, Nucl. Instrum. Methods **132**, 19 (1976).
[19] H. D. Betz, Rev. Mod. Phys. **44**, 465 (1972).
[20] R. A. Baragiola, P. Ziem, and N. Stolterfoht, J. Phys. B **9**, L447 (1976).
[21] H. D. Betz, R. Schramm, and W. Oswald, in *Interaction of Charged Particles with Solids and Surfaces*, edited by A. Gras-Marti, H. M. Urbassek, N. R. Arista, and F. Flores (Plenum, New York, 1991).
[22] R. Schramm and H. D. Betz, Nucl. Instrum. Methods Phys. Res. B **69**, 123 (1992).
[23] A. F. Lifschitz and N. R. Arista, Phys. Rev. A **69**, 012902 (2004).
[24] P. H. Mokler and F. Folkmann, in *Structure and Collisions of Ions and Atoms*, edited by I. A. Sellin (Springer-Verlag, Berlin, 1978), p. 201.
[25] M. Pajek *et al.*, AIP Conf. Proc. **475**, 32 (1999).
[26] D. Banaś *et al.*, Nucl. Instrum. Methods Phys. Res. B **195**, 233 (2002).
[27] U. Majewska, J. Braziewicz, M. Polasik, K. Słabkowska, I. Fijał, M. Jaskóła, A. Korman, S. Chojnacki, and W. Kretschmer, Nucl. Instrum. Methods Phys. Res. B **205**, 799 (2003).
[28] D. Banaś, J. Braziewicz, U. Majewska, M. Pajek, J. Semaniak, T. Czyżewski, M. Jaskóła, W. Kretschmer, and T. Mukoyama, Nucl. Instrum. Methods Phys. Res. B **154**, 247 (1999).
[29] D. Banaś, J. Braziewicz, A. Kubala Kukuś, U. Majewska, M. Pajek, J. Semaniak, T. Czyżewski, M. Jaskóła, W. Kretschmer, and T. Mukoyama, Nucl. Instrum. Methods Phys. Res. B **164**, 344 (2000).
[30] D. Banaś, J. Braziewicz, U. Majewska, M. Pajek, J. Semaniak, T. Czyżewski, M. Jaskóła, W. Kretschmer, T. Mukoyama, and D. Trautmann, J. Phys. B **33**, L793 (2000).
[31] U. Majewska, K. Słabkowska, M. Polasik, J. Braziewicz, D. Banaś, T. Czyżewski, I. Fijał, M. Jaskóła, A. Korman, and S. Chojnacki, J. Phys. B **35**, 1941 (2002).
[32] U. Majewska, J. Braziewicz, D. Banaś, M. Jaskóła, T. Czyżewski, W. Kretschmer, K. Słabkowska, F. Pawłowski, and M. Polasik, Acta Phys. Pol. B **31**, 511 (2000).
[33] J. Braziewicz, U. Majewska, M. Polasik, K. Słabkowska, I. Fijał, M. Jaskóła, A. Korman, and W. Kretschmer, Nucl. Instrum. Methods Phys. Res. B **235**, 403 (2005).

[34] J. Braziewicz, U. Majewska, K. Słabkowska, M. Polasik, I. Fijał, M. Jaskóła, A. Korman, W. Czarnacki, S. Chojnacki, and W. Kretschmer, Phys. Rev. A **69**, 062705 (2004).
[35] K. Shima, T. Ishihara, and T. Mikumo, Nucl. Instrum. Methods **200**, 605 (1982).
[36] G. Schiwietz and P. L. Grande, Nucl. Instrum. Methods Phys. Res. B **175-177**, 125 (2001).
[37] J. P. Biersack and L. G. Haggmark, Nucl. Instrum. Methods **174**, 257 (1980).
[38] J. Ziegler, [http://www.srim.org].
[39] M. Pajek, A. P. Kobzev, R. Sandrik, R. A. Ilkhamov, and S. A. Khusmorodov, Nucl. Instrum. Methods Phys. Res. B **42**, 346 (1989).
[40] H. Tawara, P. Richard, and K. Kawatsura, Phys. Rev. A **26**, 154 (1982).
[41] F. Biggs, L. B. Mendelsohn, and J. B. Mann, At. Data Nucl. Data Tables **16**, 201 (1975).
[42] M. Polasik, Phys. Rev. A **39**, 616 (1989).
[43] M. Polasik, Phys. Rev. A **39**, 5092 (1989).
[44] M. Polasik, Phys. Rev. A **40**, 4361 (1989).
[45] M. Polasik, Phys. Rev. A **41**, 3689 (1990).
[46] M. Polasik, Phys. Rev. A **52**, 227 (1995).
[47] M. Polasik, Phys. Rev. A **58**, 1840 (1998).
[48] M. Polasik, S. Raj, B. B. Dhal, H. C. Padhi, A. K. Saha, M. B. Kurup, K. G. Prasad, and P. N. Tandon, J. Phys. B **32**, 3711 (1999).
[49] M. W. Carlen *et al.*, Phys. Rev. A **46**, 3893 (1992).
[50] M. W. Carlen, B. Boschung, J.-Cl. Dousse, Z. Halabuka, J. Hoszowska, J. Kern, Ch. Rhême, M. Polasik, P. Rymuza, and Z. Sujkowski, Phys. Rev. A **49**, 2524 (1994).
[51] B. B. Dhal, H. C. Padhi, K. G. Prasad, P. N. Tandon, and M. Polasik, J. Phys. B **31**, 1225 (1998).
[52] B. J. McKenzie, I. P. Grant, and P. H. Norrington, Comput. Phys. Commun. **21**, 233 (1980).
[53] I. P. Grant, J. Phys. B **7**, 1458 (1974).
[54] P. M. Echenique, F. Flores, and R. H. Ritchie, in *Solid State Physics: Advances in Research and Applications*, edited by H. Ehrenreich (Academic Press, New York, 1990), Vol. 43, pp. 229–308.
[55] P. Bauer, F. Kastner, A. Arnau, A. Salin, P. D. Fainstein, V. H. Ponce, and P. M. Echenique, Phys. Rev. Lett. **69**, 1137 (1992).
[56] A. Arnau, P. Bauer, F. Kastner, A. Salin, V. H. Ponce, P. D. Fainstein, and P. M. Echenique, Phys. Rev. B **49**, 6470 (1994).
[57] J. Burgdörfer, Nucl. Instrum. Methods Phys. Res. B **67**, 1 (1992).
[58] J. D. Fuhr, V. H. Ponce, F. J. García de Abajo, and P. M. Echenique, Phys. Rev. B **57**, 9329 (1998).
[59] K. Słabkowska and M. Polasik, Nucl. Instrum. Methods Phys. Res. B **205**, 123 (2003).
[60] M. Kavčič *et al.*, Phys. Rev. A **61**, 052711 (2000).
[61] J. A. Bearden, Rev. Mod. Phys. **39**, 78 (1967).
[62] V. S. Nikolaev and I. S. Dmitriev, Phys. Lett. A **28**, 277 (1968).
[63] E. Baron and B. Delaunay, Phys. Rev. A **12**, 40 (1975).
[64] Ph. Deschepper, P. Lebrun, J. Lehmann, L. Palffy, and P. Pellergin, Nucl. Instrum. Methods **166**, 531 (1979).
[65] K. X. To and R. Drouin, Phys. Scr. **14**, 277 (1976).
[66] K. X. To and R. Drouin, Nucl. Instrum. Methods **160**, 461 (1979).
[67] E. Baron, J. Phys. Colloques C1 Suppl. **40**, 163 (1979).
[68] Y. Baudinet-Robinet, Nucl. Instrum. Methods **190**, 197 (1981).
[69] W. Brandt and G. Lapicki, Phys. Rev. A **20**, 465 (1979); **23**, 1717 (1981).
[70] V. S. Nikolaev, Zh. Eksp. Teor. Fiz. **51**, 1263 (1966); Sov. Phys. JETP **24**, 847 (1967).
[71] G. Lapicki and F. D. McDaniel, Phys. Rev. A **22**, 1896 (1980).
[72] R. K. Gardner, T. J. Gray, P. Richard, C. Schmiedekamp, K. A. Jamison, and J. M. Hall, Phys. Rev. A **15**, 2202 (1977).
[73] C. L. Cocke, S. L. Varghese, and B. Curnutte, Phys. Rev. A **15**, 874 (1977).